Direct Observation of Nondiffusive Motion of a Brownian Particle

B. Lukić,[1] S. Jeney,[1] C. Tischer,[2] A. J. Kulik,[1] L. Forró,[1] and E.-L. Florin[3,*]

[1]*Institut de Physique de la Matière Complexe, Ecole Polytechnique Fédérale de Lausanne (EPFL), CH-1015 Lausanne, Switzerland*
[2]*European Molecular Biology Laboratory, Meyerhofstrasse 1, D-69117 Heidelberg, Germany*
[3]*Center for Nonlinear Dynamics, University of Texas, Austin, Texas 78712, USA*

(Received 18 June 2005; published 11 October 2005)

The thermal position fluctuations of a *single* micron-sized sphere immersed in a fluid were recorded by optical trapping interferometry with nanometer spatial and microsecond temporal resolution. We find, in accord with the theory of Brownian motion including hydrodynamic memory effects, that the transition from ballistic to diffusive motion is delayed to significantly longer times than predicted by the standard Langevin equation. This delay is a consequence of the inertia of the fluid. On the shortest time scales investigated, the sphere's inertia has a small, but measurable, effect.

DOI: 10.1103/PhysRevLett.95.160601 PACS numbers: 05.40.Jc, 87.80.Cc

Diffusion governed by Brownian motion is an efficient transport mechanism on short time and length scales. Even a highly organized system like a living cell relies in many cases on the random Brownian motion of its constituents to fulfill complex functions. A Brownian particle will rapidly explore a heterogeneous environment that in turn strongly alters its trajectory. Thus, detailed information about the environment can be gained by analyzing the particle's trajectory. For instance, single particle rheology measures the local viscoelastic response of soft materials [1]. A thermally driven particle can image the topography of a surrounding polymer network [2]. The motion of a Brownian probe can also be used to characterize mechanical properties of molecular motors [3]. In all cases, high spatial resolution down to the nanometer scale is needed. High resolution is directly connected to the requirement to observe the motion on short time scales. For instance, a typical 1 μm size probe particle in water diffuses about 1 nm within 1 μs. However, at this fast time scale, the inertia of the particle and the surrounding fluid can no longer be neglected, and one expects to see a transition from purely diffusive to ballistic motion. Thus, for complete understanding, an analysis of Brownian motion at very short time scales is necessary, taking effects of inertia into account.

The exact nature of the interaction between a Brownian particle and the surrounding fluid has been a subject of research in the last century [4–12]. As first described by Einstein [4], a Brownian particle receives momentum from the thermal fluctuations of the surrounding molecules, but its movement is damped by the viscosity of the fluid. The particle's motion can be characterized by the time evolution of the mean-square displacement $\langle \Delta x^2(t) \rangle$, which is derived from the Langevin equation:

$$m\ddot{x} = F_{\mathrm{fr}} + F_{\mathrm{th}} + F_{\mathrm{ext}}, \tag{1}$$

where m is the inertial mass of the particle, F_{fr} is the friction force, F_{th} is the force arising from random thermal fluctuations, and F_{ext} represents all external forces. For a free particle, i.e., $F_{\mathrm{ext}} = 0$, at $t \to \infty$, the motion is diffusive with $\langle \Delta x^2(t) \rangle \sim t$. For short times, when $t \to 0$, the motion becomes ballistic with $\langle \Delta x^2(t) \rangle \sim t^2$. At intermediate times, $\langle \Delta x^2(t) \rangle$ depends on the details of the interaction between the particle and its surrounding fluid. In the ballistic regime and at intermediate times, the motion is often referred to as *nondiffusive* to distinguish from the commonly known diffusive regime. The standard Langevin equation assumes that the friction force is instantaneously linear with the particle's velocity, i.e., $F_{\mathrm{fr}} \sim -\dot{x}$. However, when the particle receives momentum, it displaces the fluid in its immediate vicinity. The surrounding flow field is altered and acts back on the particle due to a non-negligible fluid inertia, as described by Hinch [6]. The friction force then includes additional terms that depend on the particle's past motion [13], which leads to a hydrodynamic memory effect and a corrected form of the Langevin equation. Such a hydrodynamic effect delays the transition from ballistic to diffusive motion, resulting in a persistence of the nondiffusive motion to much longer times.

The first indication that the standard Langevin equation does not describe Brownian motion correctly stemmed from numerical simulation of molecular motion in liquids, where ''long-time tails'' were found in the particle's velocity autocorrelation function [7]. Subsequent experiments using dynamic light scattering in colloidal suspensions [8,9] confirmed that the Brownian motion of colloidal particles is more accurately described by the corrected Langevin equation, but averaging over an ensemble of different particles was necessary and hydrodynamic interactions between particles could not be excluded [14]. Up to now, no experiment on a single particle showed quantitative agreement to the corrected theory [10–12].

In this Letter, we used a weak optical trap and interferometric particle position detection to follow directly the trajectory of a single particle in a fluid on a time scale that is sufficiently short to see nondiffusive Brownian motion. The optical trap [15] was created by focusing a 20 × -expanded Nd-YAG laser beam ($\lambda = 1064$ nm) by a

63× water-immersion objective lens (NA = 1.2, where NA is numerical aperture). Trap stiffness depends linearly on the laser power and was varied by introducing neutral density filters of different transmission coefficients into the laser beam path. A dilute suspension of microspheres was loaded into the interior of a rectangular liquid cell (size ≈2 cm × 0.5 cm and thickness ≈100 μm). We used either polystyrene (radius $a = 0.265$, 0.5, 1.205, 1.25 μm) or silica ($a = 1.2$ μm) spheres suspended in water at low concentrations to allow trapping and observation of isolated particles [16]. The light scattered by the trapped particle and the unscattered laser light are projected onto a quadrant photodiode where they form an interference pattern. A quadrant photodiode senses changes in the interference pattern that can be converted directly into a position signal. Because of the strong scattering signal, we achieve nanometer spatial and microsecond temporal resolution [17,18]. Therefore, the optical trap has a twofold function: it ensures that the particle remains within the detector range, and it provides a light source for the position detection. The lateral position fluctuations $x(t)$ of the trapped sphere were measured with an InGaAs quadrant photodiode [19]. The position signal was recorded for 2 s at 5 MHz using a low-pass filter with a cut-off frequency at 1 MHz, amplified and digitized (12 bits). The effective sampling rate f_s was 500 kHz; such high oversampling avoids aliasing artifacts in data acquisition [20]. A constant offset from the high-frequency noise of the laser source and the detection system was subtracted from the calculated $\langle \Delta x^2(t) \rangle$ [21].

In our experiment, the particle was confined inside a weak and harmonic optical trapping potential, which adds a force term $F_{\text{ext}} = -kx$ to the Langevin equation, where k is the trap stiffness. In order to estimate k [22], we calibrated the detector sensitivity using the standard Langevin theory, as commonly done [23]. This method introduced a systematic error in the form of a multiplicative factor, but was nevertheless sufficiently accurate to evaluate how the mean-square displacement $\langle \Delta x^2(t) \rangle$ is influenced by the confinement of the trapping potential.

Figure 1 shows $\langle \Delta x^2(t) \rangle$ calculated from one-dimensional time traces of the largest polystyrene microsphere ($a = 1.25$ μm), over five decades of time for three different trap stiffnesses. In comparison, the dashed line in Fig. 1 indicates how $\langle \Delta x^2(t) \rangle$ would evolve if the particle was performing free and diffusive Brownian motion. The theoretical expectation is $\langle \Delta x^2(t) \rangle = 2Dt$, with the diffusion coefficient $D = k_B T/(6\pi\eta a)$, where η is the viscosity of the fluid. However, a particle in an optical trap experiences an additional drift towards the trap center due to F_{ext}. The position autocorrelation time of the particle motion $\tau_{\text{trap}} = 6\pi\eta a/k$ describes the time scale on which F_{ext} makes the particle return from a displaced position to the trap center. For the softest trap (k_1), $\tau_{\text{trap}} =$ 20 ms; for the stiffest trap (k_3), $\tau_{\text{trap}} = 1$ ms. As seen in the three data sets in Fig. 1, for $t \gg \tau_{\text{trap}}$, $\langle \Delta x^2(t) \rangle$ approaches a constant value that is inversely proportional to the trap stiffness as $\langle \Delta x^2(\infty) \rangle = 2k_B T/k$. For $t \cong \tau_{\text{trap}}$, the trapping force-induced drift causes $\langle \Delta x^2(t) \rangle$ of the displaced particle to be smaller than that of a free particle. For $t \ll \tau_{\text{trap}}$, the fluctuations of the sphere approach that of a free particle independent of its position in the trap [24]. Furthermore, at times below 10^{-4} s, Fig. 1 shows that the motion starts to deviate from the diffusive regime. In order to study this free and nondiffusive motion in greater detail, we used the softest trap and analyzed $\langle \Delta x^2(t) \rangle$ on time scales that were two decades below τ_{trap}, where the influence of F_{ext} is negligible [25].

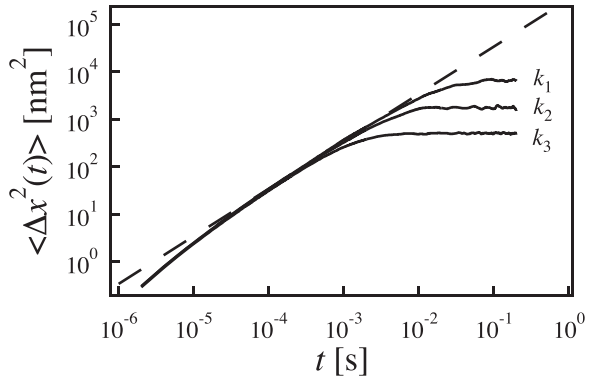

FIG. 1. Calculated $\langle \Delta x^2(t) \rangle$ for a polystyrene sphere ($a = 1.25$ μm) in the optical trap at various stiffnesses (continuous lines, $k_1 = 1.2$, $k_2 = 4.4$, and $k_3 = 16$ μN/m). The dashed curve indicates free Brownian motion in the diffusive regime when $\langle \Delta x^2(t) \rangle = 2Dt$.

We use the dimensionless representation $\langle \Delta x^2(t) \rangle/(2Dt)$ to distinguish between the diffusive regime when $\langle \Delta x^2(t) \rangle/(2Dt) = 1$ and the nondiffusive regime when $\langle \Delta x^2(t) \rangle/(2Dt) < 1$. In the standard Langevin equation a fast exponential transition from the ballistic to the diffusive regime occurs with

$$\frac{\langle \Delta x^2(t) \rangle}{2Dt} = 1 + \frac{\tau_p}{t}(e^{-t/\tau_p} - 1), \tag{2}$$

where $\langle \Delta x^2(t) \rangle$ scales with the characteristic time $\tau_p = m/(6\pi\eta a) = \frac{2}{9} a^2 \rho_p/\eta$, and ρ_p is the density of the particle. The corrected Langevin equation results in a slower algebraic transition with [9]

$$\frac{\langle \Delta x^2(t) \rangle}{2Dt} = 1 - 2\sqrt{\frac{1}{\pi}\frac{\tau_f}{t}} + \frac{8}{9}\frac{\tau_f}{t} - \frac{\tau_p}{t} + \Xi\left(\frac{\tau_p}{\tau_f}, \frac{t}{\tau_f}\right), \tag{3}$$

where $\langle \Delta x^2(t) \rangle$ depends additionally on $\tau_f = a^2 \rho_f/\eta$, where ρ_f is the density of the fluid. $\Xi(\frac{\tau_p}{\tau_f}, \frac{t}{\tau_f})$ is a small correction term [26]. Both equations are dependent on the particle's inertia through the time τ_p, but the second equation also accounts for the fluid's inertia through the characteristic time τ_f. The 2 times are related by the relation

$\tau_p/\tau_f = \frac{2}{9}\rho_p/\rho_f$. The only difference between Eqs. (2) and (3) is that they were derived assuming different friction laws (note that the friction force does not depend on ρ_p, but only on a and ρ_f [13]). By neglecting the particle's inertia, τ_p approaches zero and the nondiffusive terms disappear in Eq. (2). In Eq. (3) the nondiffusive motion persists due to the term that contains the characteristic time τ_f, which corresponds to the time taken by the perturbed flow field to diffuse over a distance of one particle's radius. The standard Langevin equation does not assume any perturbation of the fluid due to the motion of the Brownian particle, and hence τ_f does not appear in Eq. (2).

In order to study the influence of the fluid's inertia, we tracked the Brownian motion of particles with the same density (polystyrene, $\rho_p/\rho_f = 1.06$) but different radii [27]. This effect is equivalent to varying both τ_f and τ_p, while keeping τ_p/τ_f constant. Figure 2 shows the time evolution of $\langle \Delta x^2(t)\rangle/(2Dt)$, as well as the experimental data as obtained from single time traces of three different sphere sizes ($a = 0.265$, 0.5, 1.25 μm). Equation (3) was fitted to the data for times $t < 150\tau_f$, with one fitting parameter—a multiplicative factor corresponding to the detector sensitivity [28]. Since the time in Fig. 2 is normalized with τ_f, spheres with the same density but different sizes fall on the same curve. Although all three data sets have the same temporal resolution of $1/f_s = 2$ μs, they sample different regions of the theoretical curve due to their different values of τ_f ($\tau_f = 0.07$, 0.25, 1.56 μs, respectively). Larger spheres go to lower values of t/τ_f, and data points are more closely spaced on the graph. The theory agrees with the data within 2%, and the same accuracy was obtained for measurements with 10 different spheres.

The influence of the particle's inertia can be determined by comparing the position fluctuations of particles of the same size but different densities, as shown in Fig. 3. We again fitted Eq. (3) (continuous lines) to the data. Here, inertias of the two particles are different (different τ_p), but the inertia of the perturbed fluid stays the same (same τ_f). The data for the two particles differ from each other by only 6% for the shortest times measured. Thus, for $t \cong \tau_f$, the fluid's inertia influences the Brownian motion more than the particle's inertia. A single curve on which all data fall cannot be obtained by normalizing time with τ_f or τ_p, since the ratio τ_p/τ_f is not constant. In contrast, the standard Langevin equation (dashed lines) gives the same master curve for curves with different particle densities ρ_p, when scaled with τ_p (inset), as expected from Eq. (2). The corrected Langevin equation thus predicts two phenomena operating on different time scales that can influence the motion of a Brownian particle.

In the corrected model of Brownian motion [6], the thermally excited fluid molecules give momentum to the particle which is further redistributed between the particle and the surrounding fluid. Because the fluid has been displaced by the particle, the momenta of the fluid molecules are not randomly distributed, and when the particle slows down due to the fluid, the frictional force has not yet attained its steady-state value. The motion of the surrounding fluid thus contains information of the particle's past motion. We can infer from Eq. (3) that this hydrodynamic memory influences the particle's motion up to times on the order of $10^4\tau_f$. However, in our experiments, for this time

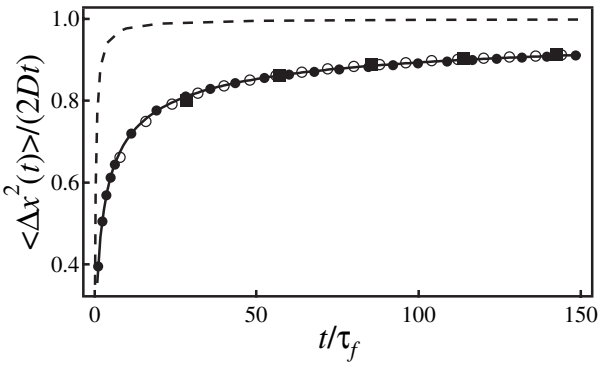

FIG. 2. The corrected Langevin theory (continuous line) is fitted to the experimental data for three different radii of a polystyrene sphere ($a = 0.265$ μm, ■; 0.5 μm, ○; 1.25 μm, ●). The standard Langevin theory is plotted as a dashed line for comparison. (For the largest sphere some data points were removed for clarity.)

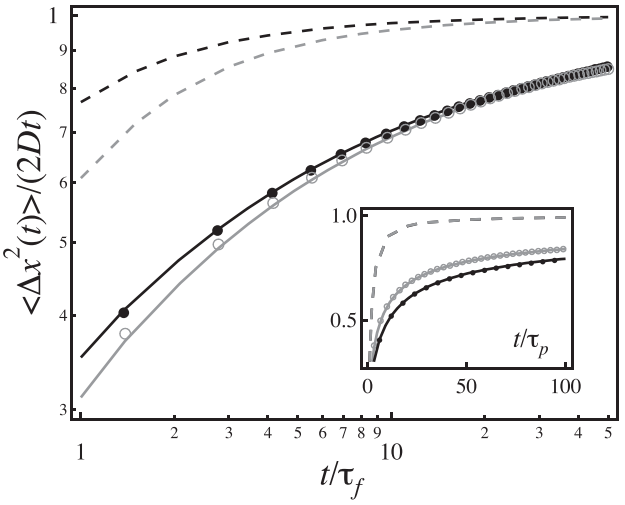

FIG. 3. Comparison of the nondiffusive motion of particles with the same radius and different densities. Theory and experimental data for spheres made of polystyrene ($\rho_p/\rho_f = 1.06$) are colored in black and for those made of silica ($\rho_p/\rho_f = 1.96$) in gray. The standard and the corrected Langevin theory are plotted as dashed and continuous lines, respectively. Experimental data are represented as ○ for silica ($a = 1.2$ μm) and as ● for polystyrene ($a = 1.205$ μm). Time is divided by τ_f ($\tau_f = 1.44$ μs). Inset: The same data, but time is scaled with τ_p.

scale, the motion is already dominated by the optical trap as shown in Fig. 1 [29].

In summary, we observed the transition regime between ballistic and diffusive motion of a single particle in an optical trap and found excellent agreement with the Langevin equation corrected for the inertia of the surrounding fluid. The fluid inertia dominates the response in the nondiffusive regime. A small contribution expected from the particle's inertia could still be quantified. This study underlines that deviations from the standard Langevin theory, due to the fluid inertia and the resulting hydrodynamic memory effect, become increasingly important when high-resolution experiments are performed.

Our method allows studying details of the mobility of Brownian particles in heterogeneous environments such as complex fluids or living cells that were previously not accessible. Ultimately, the achieved precision may address principles governing particle motion in cells and other physical systems where energies are comparable to $k_B T$.

We are grateful to J. Lekki for help in data acquisition, to T. Feher for help in fast data analysis, and to A. Jonas and Ž. Sviben for discussions. B. L. acknowledges the financial support of the National Center for Competence in Research "Nanoscale Science" of the Swiss National Science Foundation. We thank EPFL for funding the experimental equipment.

*Electronic address: florin@chaos.utexas.edu

[1] F. C. MacKintosh and C. F. Schmidt, Curr. Opin. Colloid Interface Sci. **4**, 300 (1999).

[2] C. Tischer, S. Altmann, S. Fisinger, J. K. H. Hörber, E. H. K. Stelzer, and E.-L. Florin, Appl. Phys. Lett. **79**, 3878 (2001).

[3] S. Jeney, E. H. K. Stelzer, H. Grubmüller, and E.-L. Florin, Chem. Phys. Chem. **5**, 1150 (2004).

[4] A. Einstein, Ann. Phys. (Leipzig) **17**, 549 (1905).

[5] V. Vladimirsky and Ya. Terletzky, Zh. Eksp. Teor. Fiz. **15**, 259 (1945). Here one finds the first analytical solution of the corrected form of the Lagevin equation. It is equivalent to that in Ref. [6] (V. Lisy and J. Tohtova, cond-mat/0410222).

[6] E. J. Hinch, J. Fluid Mech. **72**, 499 (1975).

[7] A. Rahman, Phys. Rev. **136**, A405 (1964); B. J. Alder and T. E. Wainwright, Phys. Rev. Lett. **18**, 988 (1967).

[8] J. P. Boon and A. Bouiller, Phys. Lett. **55A**, 391 (1976); G. L. Paul and P. N. Pusey, J. Phys. A **14**, 3301 (1981); K. Ohbayashi, T. Kohno, and H. Utiyama, Phys. Rev. A **27**, 2632 (1983).

[9] D. A. Weitz, D. J. Pine, P. N. Pusey, and R. J. A. Tough, Phys. Rev. Lett. **63**, 1747 (1989); J. X. Zhu, D. J. Durian, J. Muller, D. A. Weitz, and D. J. Pine, Phys. Rev. Lett. **68**, 2559 (1992); M. H. Kao, A. G. Yodh, and D. J. Pine, Phys. Rev. Lett. **70**, 242 (1993).

[10] Y. W. Kim and J. E. Matta, Phys. Rev. Lett. **31**, 208 (1973); P. D. Fedele and Y. W. Kim, Phys. Rev. Lett. **44**, 691 (1980).

[11] A. Meller, R. Bar-Ziv, T. Tlusty, E. Moses, J. Stavans, and S. A. Safran, Biophys. J. **74**, 1541 (1998).

[12] E. J. G. Peterman, M. A. van Dijk, L. C. Kapitein, and C. F. Schmidt, Rev. Sci. Instrum. **74**, 3246 (2003).

[13] Friction force now has terms that depend on $\ddot{x}$ as well, giving $F_{\rm fr}(t) = -6\pi\eta a\dot{x} - \frac{2}{3}\pi a^3\rho_f\ddot{x} - 6a^2\sqrt{\pi\rho_f\eta}\times \int_0^t (t-t')^{-1/2}\ddot{x}(t')dt'$, where a is the radius of the particle, and ρ_f density and η viscosity of the fluid. H. J. H. Clercx and P. P. J. M. Schram, Phys. Rev. A **46**, 1942 (1992).

[14] S. Henderson, S. Mitchell, and P. Bartlett, Phys. Rev. Lett. **88**, 088302 (2002).

[15] A. Ashkin, J. M. Dziedzic, J. E. Bjorkholm, and S. Chu, Opt. Lett. **11**, 288 (1986).

[16] The concentration c determines the average shortest distance $\bar{r}$ between particles in solution. For the simplest case of particles arranged in a regular lattice, the relation between the two quantities is given by $\bar{r} = c^{-1/3}$. Two particles separated by a distance r interact hydrodynamically via diffusion of their respective flow fields. Hence, one particle is isolated from its neighbor only for times smaller than the time $r^2\rho_f/\eta$ it takes for its flow field to propagate over the distance r. Here, we chose c on the order of 10^6 spheres/mL such that $\bar{r}^2\rho_f/\eta$ was on the order of 10 ms.

[17] F. Gittes and C. F. Schmidt, Opt. Lett. **23**, 7 (1998).

[18] A. Pralle, M. Prummer, E.-L. Florin, E. H. K. Stelzer, and J. K. H. Hörber, Microsc. Res. Tech. **44**, 378 (1999).

[19] A. Rohrbach, C. Tischer, D. Neumayer, E.-L. Florin, and E. H. K. Stelzer, Rev. Sci. Instrum. **75**, 2197 (2004).

[20] K. Berg-Sørensen and H. Flyvbjerg, Rev. Sci. Instrum. **75**, 594 (2004).

[21] See EPAPS Document No. E-PRLTAO-95-035542 for a detailed description of signal acquisition. This document can be reached via a direct link in the online article's HTML reference section or via the EPAPS homepage (http://www.aip.org/pubservs/epaps.html).

[22] E.-L. Florin, A. Pralle, E. H. K. Stelzer, and J. K. H. Hörber, Appl. Phys. A **66**, S75 (1998).

[23] F. Gittes and C. F. Schmidt, Methods Cell Biol. **55**, 129 (1998).

[24] C. Tischer, A. Pralle, and E.-L. Florin, Microsc. Microanal. **10**, 425 (2004).

[25] A full description of the motion of a Brownian particle in an optical trap, including the interplay of $F_{\rm ext}$ and $F_{\rm fr}$, will be published elsewhere.

[26] Equation (3) is exact with $\Xi(\frac{\tau_p}{\tau_f}, \frac{t}{\tau_f}) = \frac{3}{t(5\tau_f - 36\tau_p)^{1/2}}\times [\frac{1}{\alpha_+^3} e^{\alpha_+^2 t}\,\mathrm{erfc}(\alpha_+\sqrt{t}) - \frac{1}{\alpha_-^3} e^{\alpha_-^2 t}\,\mathrm{erfc}(\alpha_-\sqrt{t})]$, where $\alpha_\pm = \frac{3}{2}\frac{3\pm(5-36\tau_p/\tau_f)^{1/2}}{\sqrt{\tau_f}(1+9\tau_p/\tau_f)}$.

[27] For our experiments performed in water, $\rho_f = 1000\ \mathrm{kg/m^3}$ and $\eta = 0.001$ Pa s.

[28] The data are hence independent of any assumptions needed for the calibration of the instrument.

[29] For a sphere with a radius of 1.25 μm in the softest trap ($k_1 = 1.2\ \mu\mathrm{N/m}$), $10^4\tau_f \cong 16$ ms is on the same order as $\tau_{\rm trap} = 20$ ms.